Electronic Supplementary Material (ESI) for ChemComm.

The assembly of $[Mo_2O_2S_2]^{2+}$ based on polydentate phosphonate templates and their proton conductivity

Bo Li,[a†] Yu-Xi Meng,[a†] Qian-Qian Liu,[a] Xin-Yu Chen,[a] Xin Liu,[a] and Hong-Ying Zang[*a]

[a] Key Laboratory of Polyoxometalate Science, Department of Chemistry, Northeast Normal University, Ren Min Street No. 5268, Changchun, Jilin, 130024, P. R. China.

E-mail: zanghy100@nenu.edu.cn

† B.Li and Y. Meng contributed equally.

1. Materials and methods

All obtained reagents, including amino trimethylene phosphonic acid (ATMP), ethylene diamine tetra (methylene phosphonic acid) (EDTMPA), potassium carbonate and ammonium molybdate were all commercially available and were purified without further purification. Oxothio dimer $[Mo_2S_2O_2(H_2O)_6]^{2+}$ was synthesized according to the literature[1]. Powder X-ray diffraction (PXRD) measurement was recorded ranging from 5 to 50° at room temperature on a Siemens D5005 diffractometer with Mo-Kα (λ = 0.71073 Å). The crystallographic diffraction data were collected at 293 K on Bruker Apex II with Mo Kα (λ = 0.71073 Å). IR spectrum was performed using a Nicolet Magna 560 IR spectrometer with a wavelength range of 4000-400 cm^{-1}, with KBr pellets. Differential Thermogravimetric Analysis (TGA) is performed in a nitrogen atmosphere on TA Instruments Simultaneous DSC-TGA Q SeriesTM, the temperature range is 25-800℃ with a heating rate of 10 ℃ min^{-1}. ICP-OES elemental analyses were performed on ICP-OES Leeman Prodigy. C, H, S and N elemental analyses were performed by using a Eurovec-tor EA3000 elemental analyzer. ^{31}P NMR spectra were recorded on Bruker 500 MHz instrument. Water vapor adsorption were performed by using a 3H-2000PW Multi-station Gravimetric Vapor Sorption Apparatus.

2. Synthesis and Characterization

Synthesis of $K_2H_{16}\{(Mo_2O_2S_2)_{10}(OH)_{14}[N(CH_2PO_3)_3]_4\}\cdot 60H_2O$

$[Mo_2S_2O_2]^{2+}$ was synthesized following the procedure outlined in a previous reference [24]. Amino trimethylene phosphonic acid (0.105g, 0.35 mmol) was dissolved in 10 mL of deionized water, and the pH was adjusted to 7.0 using 1M K_2CO_3. The mixture was stirred for 10 minutes. Subsequently, 7.4 mL of $[Mo_2S_2O_2]^{2+}$ solution was dissolved in 10 mL of deionized water and slowly added to the aforementioned solution. The pH was then adjusted to 4.5 using 1M K_2CO_3, resulting in an orange-red clear solution. After stirring at room temperature for 1 hour, the solution was filtered. The obtained filtrate was subjected to conventional evaporation for two weeks, yielding red rod-like crystals. Element analyses (%) calcd for $C_{12}H_{144}K_2Mo_{20}N_4O_{130}P_{12}S_{20}$; H, 3.20, Mo, 35.10, S, 11.73, P, 6.80, K, 1.43; Found: H, 2.95, Mo, 35.74, S, 11.83, P, 6.27, K, 1.75.

Synthesis of $K_{12}\{(Mo_2O_2S_2)_8(OH)_{12}[N_2C_2H_4(CH_2PO_3)_4]_2\}\cdot 40H_2O$

Ethylenediamine tetramethylene phosphonic acid (0.245 g, 0.56 mmol) was dissolved in 10 mL of deionized water, and the pH was adjusted to 7.0 using 1M K_2CO_3, resulting in a colorless and clear solution. Subsequently, 7.4 mL of $[Mo_2S_2O_2]^{2+}$ solution was dissolved in 10 ml of deionized water and slowly added to the aforementioned solution. The pH was then adjusted to 4.5 using 1M K_2CO_3, resulting in an orange-red clear solution. After stirring at room temperature for 1 hour, the solution was filtered. The filtrate was allowed to evaporate at room temperature for one week, leading to the collection of red block-shaped crystals. Element analyses (%) calcd for $C_{12}H_{116}O_{92}N_4P_8Mo_{16}S_{16}K_{12}$: H, 2.57, N, 1.23, C, 3.16, Mo, 33.7, S, 11.26, P, 5.44, K, 10.30; Found: H, 2.75, N, 1.61, C, 3.22, Mo, 33.27, S, 11.72, P, 5.18, K, 10.48.

3. Single-crystal X-ray diffraction analyses

The crystals were mounted on a Hampton cryoloop with Vaseline. Diffraction data was collected using a Bruker Apex II diffractometer with Mo-Kα radiation (λ = 0.71073 Å). The measurement temperature was 293 K. The crystal structures were solved via the SHELXT package[2] and refined using full-matrix methods against *F*^2 from Olex 2[3] software. Anisotropic refinement was performed for all non-hydrogen atoms. Crystallographic data were delivered to the Cambridge Crystallographic Data Centre (CCDC) and assigned No. 2290143 and No. 2290144.

4. Proton conductivity test

The crystalline particles of the three clusters were grounded into powder separately. The resulting powder samples were put into a mold with an inner diameter of 10 mm, and pressed into tablets under a pressure of 20 MPa for 30 seconds. The tablets were sandwiched between two gold-plated electrodes with the thickness of approximately 1.0 mm. Sanwood constant temperature and humidity chambers (SC-80-CC-3) was used to control temperature and relative humidity. The proton conductivity was measured using the alternating current (AC) impedance method of a Solartron SI 1260 Impedance/Gain Phase Analyzer, with a test frequency range of 1Hz to 1MHz and an applied voltage of 100mV. For variable temperature and variable humidity electrochemical impedance (EIS) testing, the test is performed after equilibrating each test point for 30 minutes and 12 hours, respectively. Zview software was used to fit the impedance data. Extrapolation of the arc of the impedance spectrum to the X-axis gives resistance, the proton conductivity (σ) was calculated from the resistance value (R) and the value was calculated as follows:

$$\sigma = \frac{d}{RA}$$

where d is the pellet thickness (cm), R is the resistance (Ω), A is the cross-sectional area (cm^2), respectively.

The activation energy (Ea) of $Mo_{20}(ATMP)_4$ and $Mo_{16}(EDTMP)_2$ at 80% RH was calculated from the linear Arrhenius curve, and the equation was as follows:

$$\sigma T = \sigma_0 \exp\left(\frac{-Ea}{k_B T}\right)$$

where σ_0 is the pre-exponential factor, T is the absolute temperature and k_B is the Boltzmann constant.

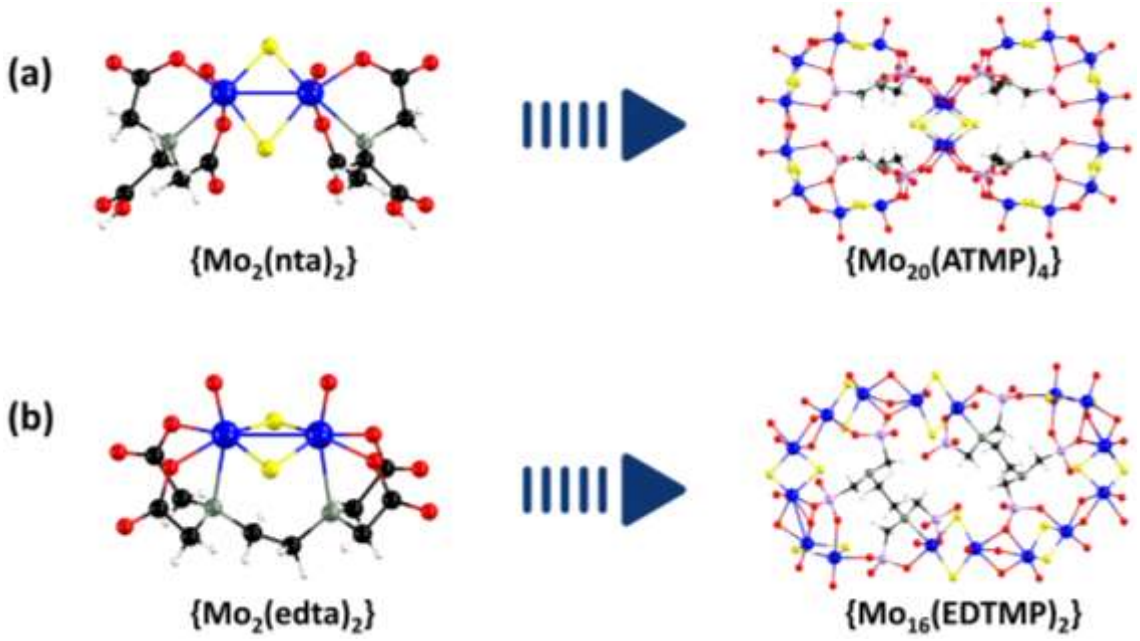

Fig. S1 The structural transformation of (a) $Mo_{20}(ATMP)_4$ (b) $Mo_{16}(EDTMP)_2$ compared to their carboxyl analog (nta= tris(carboxymethyl)amine, edta=ethylenediaminetetraacetic acid).

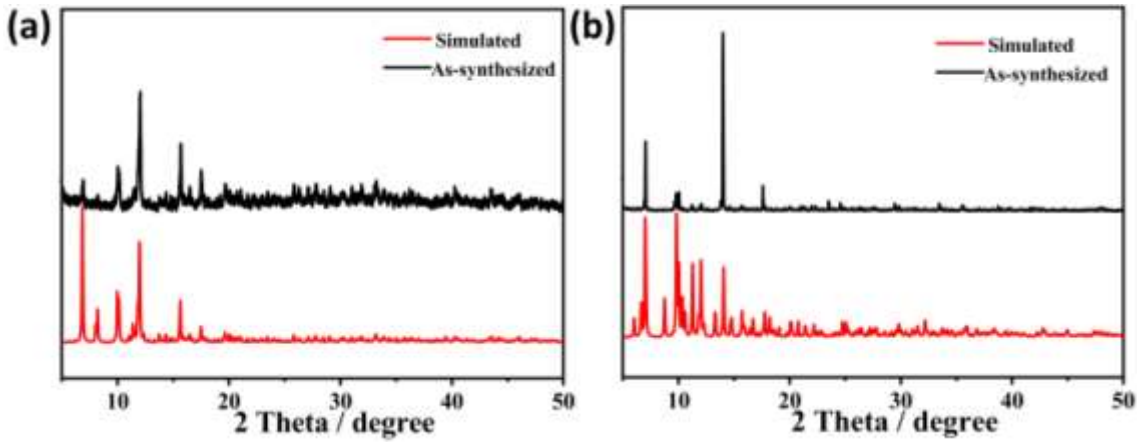

Fig. S2 PXRD patterns of (a) $Mo_{20}(ATMP)_4$ and (b) $Mo_{16}(EDTMP)_2$. The experimental spectrum closely aligns with the simulated spectrum, affirming the crystal's crystalline nature and purity, devoid of any impurities.

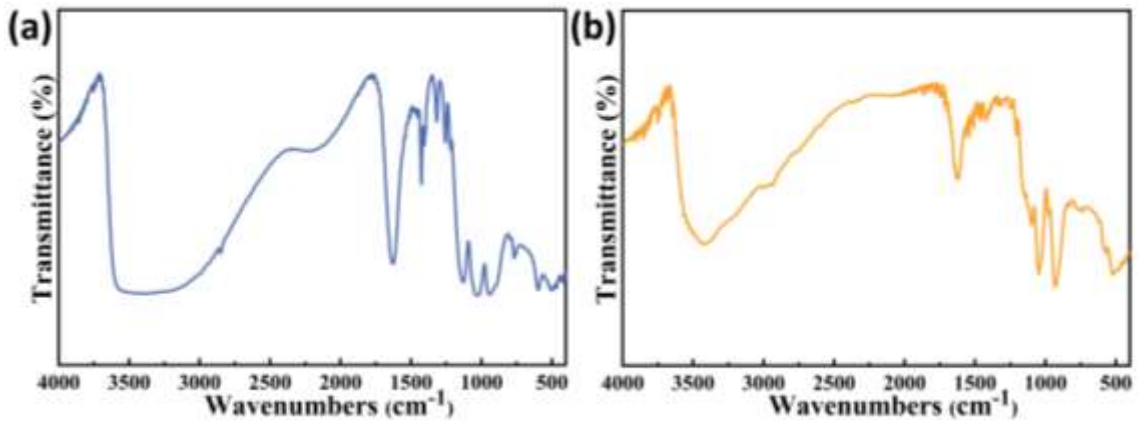

Fig. S3 FT-IR spectra of (a) $Mo_{20}(ATMP)_4$ and (b) $Mo_{16}(EDTMP)_2$. The FT-IR spectrum of $Mo_{20}(ATMP)_4$ exhibits characteristic bands at 472 cm^{-1}, 588 cm^{-1}, and 921 cm^{-1}, which should be attributed to *ν*(Mo-S-Mo), *ν*(Mo-OH-Mo), and *ν*(Mo=O), respectively.[4] The peaks at 1425 cm^{-1}, 1318 cm^{-1}, 1136 cm^{-1}, and 1040 cm^{-1} are assigned to the characteristic peaks of ATMP.[5] The peaks at 1608 cm^{-1} and 3446 cm^{-1} are attributed to the vibration and stretching of hydroxyl bending. The FT-IR spectrum of $Mo_{16}(EDTMP)_2$ exhibits characteristic bands at 515 cm^{-1}, 576 cm^{-1}, and 926 cm^{-1}, which should be attributed to *ν*(Mo-S-Mo), *ν*(Mo-OH-Mo), and *ν*(Mo=O), respectively. The peaks at 1418 cm^{-1}, 1210 cm^{-1}, 1104 cm^{-1}, and 1049 cm^{-1} are assigned to the characteristic peaks of EDTMP. The peaks at 1620 cm^{-1} and 3433 cm^{-1} are attributed to the vibration and stretching of hydroxyl bending.

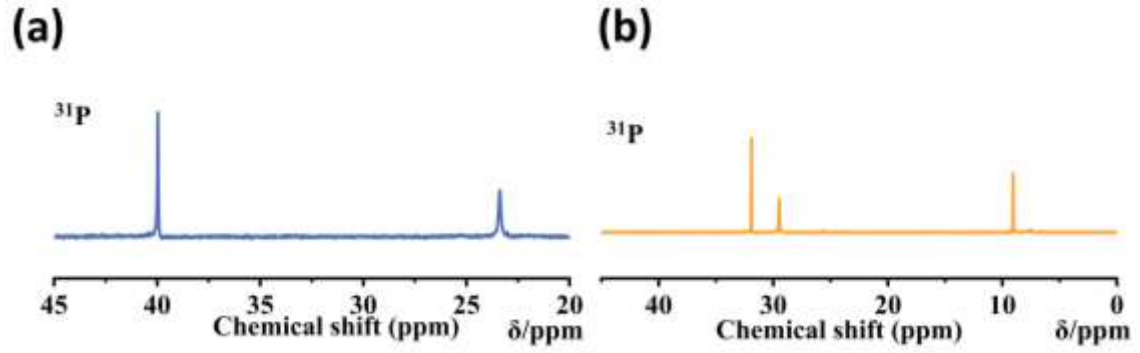

Fig. S4 ^{31}P NMR spectra of (a) $Mo_{20}(ATMP)_4$ (b) $Mo_{16}(EDTMP)_2$ tested in D_2O. The spectrum of $Mo_{20}(ATMP)_4$ reveals two resonances situated at 40.05 and 23.38 ppm. These findings are in excellent accordance with the solid-state structure of the compound, which encompasses two distinct types of P atoms within a subunit. The spectrum of $Mo_{16}(EDTMP)_2$ reveals three resonances situated at 31.88, 29.43 and 9.12 ppm, which encompasses three distinct types of P atoms within a subunit.

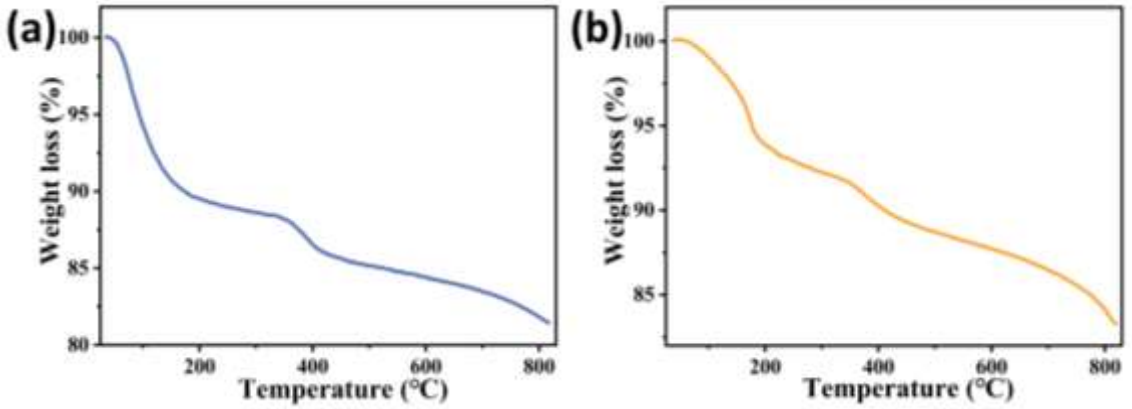

Fig. S5 Thermogravimetry analysis curves of (a) $Mo_{20}(ATMP)_4$ and (b) $Mo_{16}(EDTMP)_2$.

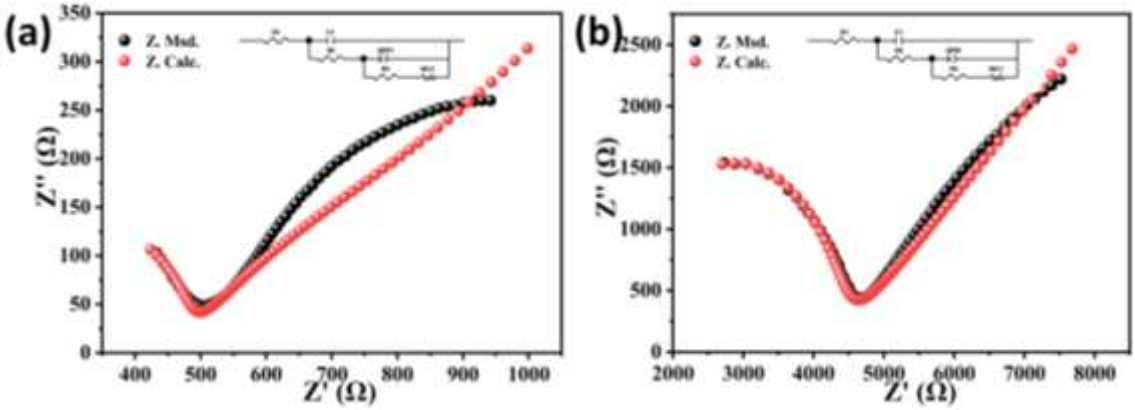

Fig. S6 The resistance value of (a) $Mo_{20}(ATMP)_4$ (b) $Mo_{16}(EDTMP)_2$ could be obtained by fitting the curves using ZsimpWin. The equivalent circuit R(C(Q(RW)))) was used to fit the impedance spectra. Z. Msd is the test plot (black) and Z.Calc is the fitting plot (red). C is capacitive processes, R is the resistance of the sample, Q is the constant phase element and W_o is the Warburg diffusion term associated with the electrode reactions.

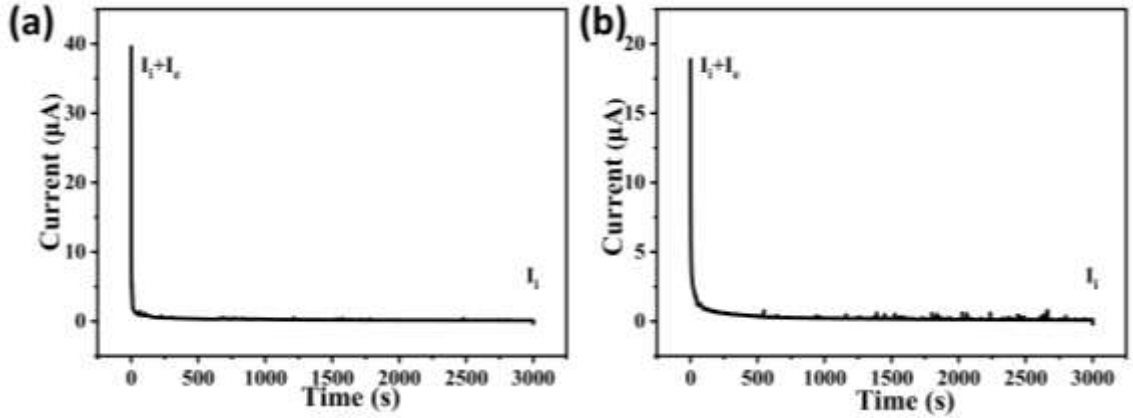

Fig. S7 Time–current relationship in the Hebb–Wagner polarization method of (a) $Mo_{20}(ATMP)_4$ (b)

$Mo_{16}(EDTMP)_2$ demonstrates that both materials exhibit proton conduction rather than electron conduction. The applied voltage is 3 V and the DC current stabilized at 0.31 μA and 0.24 μA. Electronic conductivity is 1.03×10^{-7} S cm^{-1} and 8×10^{-8} S cm^{-1}.

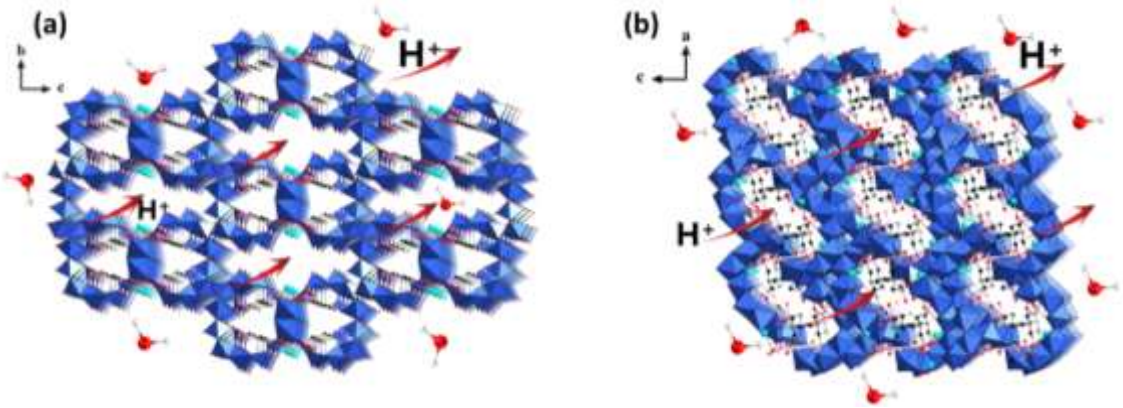

Fig. S8 Schematic diagrams of proton transport pathway in (a) $Mo_{20}(ATMP)_4$ and (b) $Mo_{16}(EDTMP)_2$.

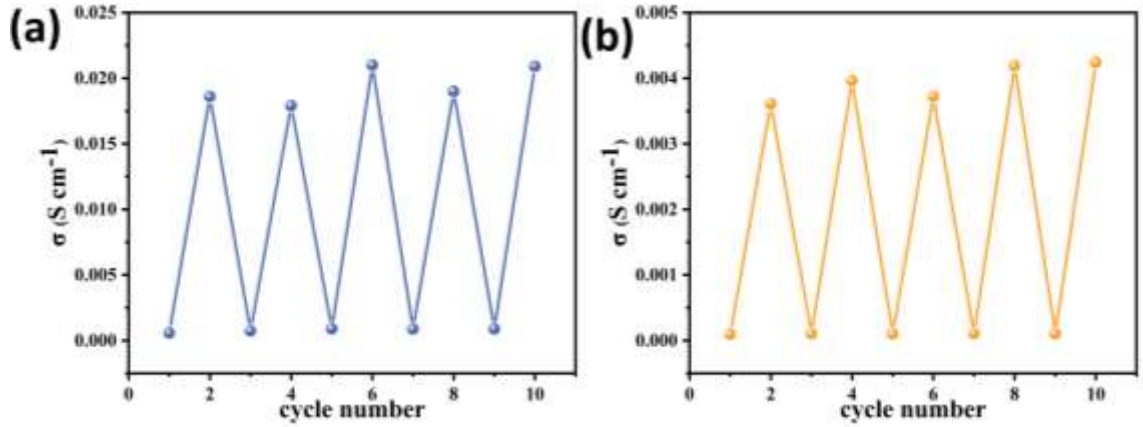

Fig. S9 Heating and cooling cycles at 30 °C and 85 °C, 80% RH.

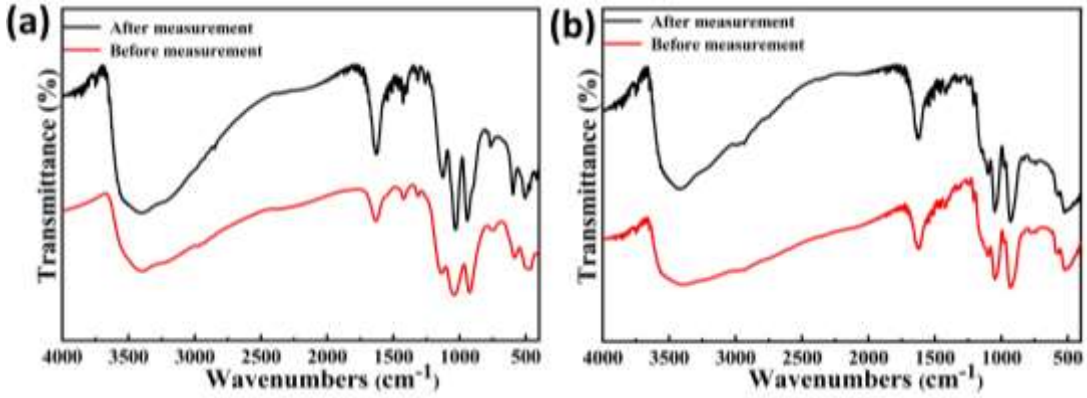

Fig. S10 FT-IR spectra of (a) $Mo_{20}(ATMP)$ (b) $Mo_{16}(EDTMP)_2$ before and after proton conduction

testing.

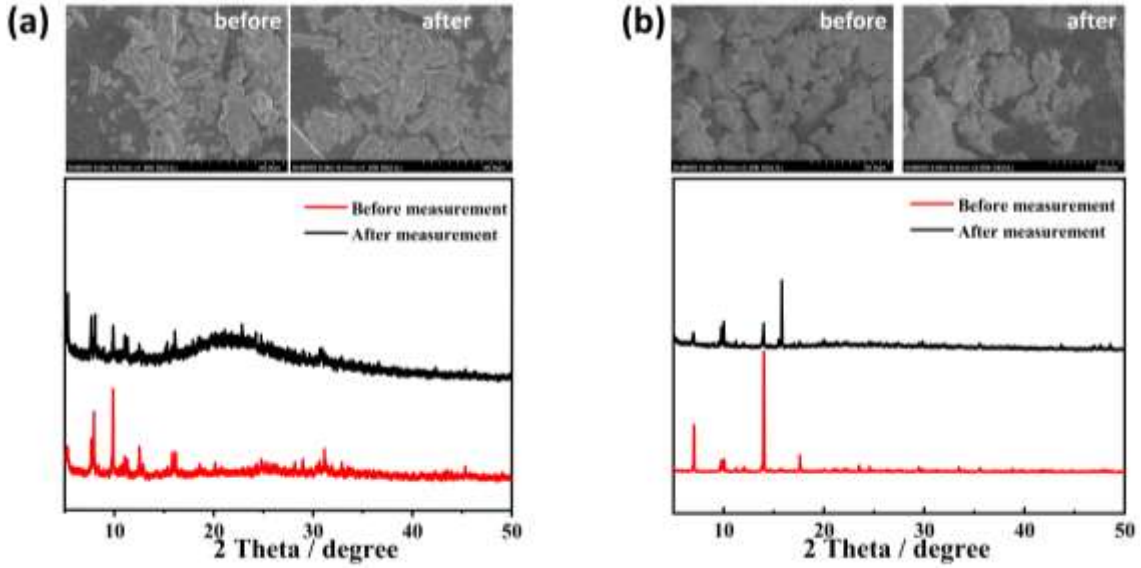

Fig. S11 XRD spectra and SEM images of (a) Mo_{20}(ATMP) (b) $Mo_{16}(EDTMP)_2$ before and after proton conduction testing.

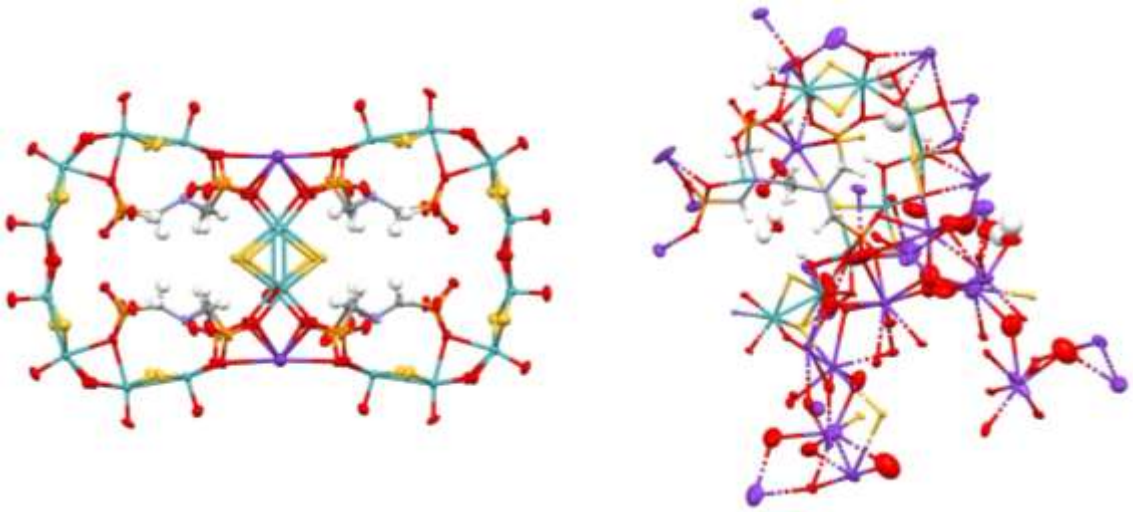

Fig. S12 The structural drawing showing the ADPs of each structure left: **$Mo_{20}(ATMP)_4$**; right: **$Mo_{16}(EDTMP)_2$**. Color code: Mo, light green; O, red; S, yellow; C, gray; N, lavender; P, orange, K, purple.

Table S1. Crystallographic data for **$Mo_{20}(ATMP)_4$**) and **$Mo_{16}(EDTMP)_2$**)

Identification code	**$Mo_{20}(ATMP)_4$**	**$Mo_{16}(EDTMP)_2$**
Empirical formula	$C_{12}H_{174}K_2Mo_{20}N_4O_{130}P_{12}S_{20}$	$C_{12}H_{116}K_{12}Mo_{16}N_4O_{92}P_8S_{16}$
Formula weight	5465.4407	4554.0709
Temperature/K	280.31	173.01
Crystal system	Orthorhombic	monoclinic
Space group	*Immm*	C2/c

a/Å	11.155(7)	29.5373(16)
b/Å	28.056(19)	17.6293(10)
c/Å	28.151(15)	25.0402(13)
α/°	90	90
β/°	90	96.514(2)
γ/°	90	90
Volume/Å^3	8810(9)	12954.8(12)
Z	2	4
ρcalcg/cm^3	1.859	2.302
μ/mm^{-1}	1.844	2.335
F(000)	4764.0	8656.0
Crystal size/mm^3	0.24 × 0.22 × 0.2	0.24 × 0.22 × 0.2
Radiation	Mo Kα (λ = 0.71073)	Mo Kα (λ = 0.71073)
2θ range for data collection/°	4.578 to 50.21	4.902 to 50.22
Index ranges	-13 ≤ h ≤ 13, -33 ≤ k ≤ 31, -30 ≤ l ≤ 33	-35 ≤ h ≤ 35, -21 ≤ k ≤ 21, -29 ≤ l ≤ 28
Reflections collected	25350	76837
Independent reflections	4258 [Rint = 0.1037, Rsigma = 0.0611]	11510 [Rint = 0.0572, Rsigma = 0.0330]
Data/restraints/parameters	4258/121/221	11510/69/824
Goodness-of-fit on F2	1.083	1.060
Final R indexes [I>=2σ (I)]	R1 = 0.0490, wR2 = 0.1173	R1 = 0.0463, wR2 = 0.1124
Final R indexes [all data]	R1 = 0.0683, wR2 = 0.1244	R1 = 0.0614, wR2 = 0.1236
Largest diff. peak/hole / e Å^{-3}	1.49/-1.00	2.25/-1.29

[a]$R_1 = \sum||F_0| - |F_C||/\sum|F_0|$; [b]$wR_2 = \sum[w(F_0^2–F_C^2)^2]/\sum[w(F_0^2)^2]^{1/2}$

Table S2. Partial bond lengths for **$Mo_{20}(ATMP)_4$**.

Atom-Atom	Length/Å	Atom-Atom	Length/Å
Mo1-Mo1^1	2.852(2)	Mo5-S1	2.316(2)
Mo1-S2^1	2.331(4)	Mo5-O1	1.680(7)
Mo1-S2^2	2.331(4)	Mo5-O10^4	2.129(5)
Mo1-S2^3	2.331(4)	Mo5-O10	2.130(5)
Mo2-Mo3	2.8248(19)	K1-O18^4	2.889(7)
Mo2-S4^4	2.309(2)	K1-O18^3	2.889(7)
Mo2-S4	2.309(2)	K1-O24	3.217(14)
Mo2-O10	2.115(5)	K1-O24^5	3.217(14)
Mo3-S4^4	2.292(2)	P1-O18	1.483(5)
Mo3-S4	2.292(2)	P1-C2	1.667(12)
Mo3-O4	1.676(7)	P1-C3	1.875(12)
Mo3-O8^4	2.079(4)	P1-O7	1.551(10)
Mo3-O8	2.079(4)	P1-O27	1.507(9)
Mo4-Mo5	2.856(2)	P2-O16	1.603(7)
Mo4-S1	2.308(2)	P2-O26	1.472(10)
Mo4-S1^4	2.308(2)	P2-C1	1.737(9)
Mo4-O6	1.669(8)	N1-C1	1.431(12)
Mo4-O12	2.109(5)	N1-C2	1.657(13)
Mo4-O12^4	2.109(5)	N1-C3^4	1.444(14)
Mo5-S1^4	2.316(2)	N1-C3	1.444(14)

[1]+X,+Y,1-Z; [2]+X,1-Y,1-Z; [3]+X,1-Y,+Z; [4]-X,+Y,+Z; [5]-X,1-Y,+Z

Table S3. Partial bond angles for **$Mo_{20}(ATMP)_4$**.

Atom-Atom-Atom	Angle/°	Atom-Atom-Atom	Angle/°
S2-Mo1-Mo1[1]	52.27(8)	O10[4]-Mo5-S1[4]	90.52(15)
S2[2]-Mo1-Mo1[1]	52.27(8)	O10-Mo5-S1[4]	154.33(15)
S2[3]-Mo1-Mo1[1]	52.27(8)	O10[4]-Mo5-O10	70.4(3)
S2[1]-Mo1-Mo1[1]	52.27(8)	O10-Mo5-O14	71.39(18)
S4-Mo2-Mo3	51.86(6)	O18[4]-K1-O24[5]	48.3(3)
S4[4]-Mo2-Mo3	51.86(6)	O18[2]-K1-O24	48.3(3)
S4-Mo2-S4[4]	103.17(12)	O18[2]-K1-O24[5]	59.4(3)
S4[4]-Mo2-O14	86.14(13)	O18[5]-K1-O24[5]	48.3(3)
S4[4]-Mo3-Mo2	52.40(6)	O12-P1-K1[4]	60.9(2)
S4-Mo3-Mo2	52.40(6)	O12-P1-C2	105.4(5)
S4[4]-Mo3-S4	104.25(12)	O12-P1-C3	102.5(5)
S4-Mo3-O16	81.33(10)	O12-P1-O7	117.4(5)
S1[4]-Mo4-Mo5	51.98(5)	Mo3-O8-Mo3[1]	107.1(3)
S1-Mo4-Mo5	51.98(5)	Mo2-O10-Mo5	99.2(2)
S1[4]-Mo4-S1	101.97(11)	Mo4-O12-K1[4]	112.5(2)
O6-Mo4-Mo5	98.3(2)	Mo4-O12-K1	112.5(2)
S1-Mo5-Mo4	51.72(5)	P1-O18-Mo1	147.0(4)
S1[4]-Mo5-Mo4	51.72(5)	P1-O18-K1	108.0(3)
S1-Mo5-S1[4]	101.49(11)	P1-O18-K1[4]	108.0(3)
O1-Mo5-Mo4	97.6(2)	Mo1-O24-K1[4]	100.3(6)

[1]+X,+Y,1-Z; [2]+X,1-Y,+Z; [3]+X,1-Y,1-Z; [4]-X,+Y,+Z; [5]-X,1-Y,+Z

Table S4. Partial bond lengths for **$Mo_{16}(EDTMP)_2$**.

Atom-Atom	Length/Å	Atom- Atom	Length/Å
Mo1-Mo4	2.8382(9)	K7-K16[8]	4.137(5)
Mo1-K12[1]	4.05(2)	K7-P8[11]	3.505(4)
Mo2-Mo4	3.2192(9)	K7-O35[7]	2.794(7)
Mo2-Mo7	2.8374(9)	K7-O48[11]	3.250(7)
Mo3-Mo8	2.8103(10)	K10-O43[8]	3.030(7)
Mo3-S3	2.343(2)	K10-O44[8]	3.103(6)
Mo4-K12[1]	4.00(3)	K11-O14	2.894(8)
Mo4-S4	2.334(2)	K11-O19	2.798(12)
Mo5-Mo6	2.8060(10)	K12-S3[8]	3.75(3)
Mo5-K7[1]	3.793(3)	K12-S4[7]	3.32(3)
Mo6-Mo8	3.2161(10)	K13-K14	4.742(11)
Mo6-K10[4]	3.687(2)	K13-P8[12]	3.533(8)
Mo7-K11	3.823(3)	K14-O5	2.87(2)
Mo7-S2	2.308(2)	K14-O9	2.79(2)
Mo8-K10[4]	3.668(2)	K15-S2[2]	3.643(14)
Mo8-K14[6]	3.998(6)	K15-O6[13]	3.312(19)
K2-K3[4]	2.97(3)	K16-O7	3.039(8)
K3-K11	4.11(2)	P4-C4	1.801(8)
K3-O13[2]	3.00(3)	P6-C1	1.822(7)
K5-K5[10]	4.950(8)	N1-C1	1.498(9)
Mo1-Mo4	2.8382(9)	K7-K16[8]	4.137(5)
Mo1-K12[1]	4.05(2)	K7-P8[11]	3.505(4)
Mo2-Mo4	3.2192(9)	K7-O35[7]	2.794(7)
Mo2-Mo7	2.8374(9)	K7-O48[11]	3.250(7)
Mo3-Mo8	2.8103(10)	K10-O43[8]	3.030(7)

[1]3/2-X,-1/2+Y,3/2-Z; [2]3/2-X,3/2-Y,2-Z; [3]3/2-X,3/2-Y,1-Z; [4]+X,2-Y,-1/2+Z; [5]1-X,+Y,3/2-Z; [6]1-X,2-Y,1-Z; [7]3/2-X,1/2+Y,3/2-Z; [8]+X,2-Y,1/2+Z; [9]3/2-X,5/2-Y,2-Z; [10]1-X,2-Y,2-Z; [11]1-X,1+Y,3/2-Z;

[12]+X,1+Y,+Z; [13]+X,1-Y,1/2+Z

Table S5. Partial bond angles for **$Mo_{16}(EDTMP)_2$**.

Atom-Atom-Atom	Angle/˚	Atom-Atom-Atom	Angle/˚
Atom-Atom-Atom	Angle/˚	Atom-Atom-Atom	Angle/˚
Mo4-Mo1-K12[1]	68.5(5)	O36-K10-O49[8]	72.9(3)
S4-Mo1-Mo4	52.56(5)	O37-K10-Mo6[8]	87.88(13)
Mo4-Mo2-K11	136.80(5)	S2-K11-S7[8]	149.74(12)
Mo7-Mo2-Mo4	144.38(3)	S7[8]-K11-Mo6[8]	37.57(5)
S3-Mo3-Mo8	52.36(5)	O37-K11-Mo7	61.87(12)
S6-Mo3-Mo8	52.46(6)	O37-K11-K15	122.6(3)
Mo1-Mo4-Mo2	129.91(3)	K13-K12-Mo4[7]	142.7(9)
Mo1-Mo4-K3[2]	150.3(4)	K14-K12-Mo1[7]	147.1(8)
Mo6-Mo5-K7[1]	142.18(10)	O36-K12-Mo4[7]	84.4(7)
Mo6-Mo5-K16[3]	82.75(4)	O36-K12-K13	126.2(9)
Mo5-Mo6-Mo8	144.74(3)	O21-K13-O39[6]	64.7(3)
Mo5-Mo6-K10[4]	150.47(5)	O21-K13-O48[12]	103.7(4)
Mo2-Mo7-K11	69.58(5)	O5-K14-K5[5]	44.1(5)
S2-Mo7-Mo2	52.29(5)	O5-K14-K10	86.0(4)
Mo3-Mo8-Mo6	133.80(3)	O39[6]-K14-K13	41.70(18)
Mo3-Mo8-K10[4]	161.24(5)	O39[6]-K14-K14[5]	107.5(2)
K3[4]-K2-S7	77.4(5)	O41[2]-K15-K2[8]	86.2(3)
O13[2]-K3-O17[9]	77.5(6)	O8-P1-O22	108.9(3)
O15-K5-K5[10]	119.6(3)	K16-O6-K15[16]	136.3(4)
Mo5[7]-K7-K16[8]	57.94(6)	Mo1-O12-Mo5	109.1(2)

[1]3/2-X,-1/2+Y,3/2-Z; [2]3/2-X,3/2-Y,2-Z; [3]3/2-X,3/2-Y,1-Z; [4]+X,2-Y,-1/2+Z; [5]1-X,+Y,3/2-Z; [6]1-X,2-Y,1-Z; [7]3/2-X,1/2+Y,3/2-Z; [8]+X,2-Y,1/2+Z; [9]3/2-X,5/2-Y,2-Z; [10]1-X,2-Y,2-Z; [11]1-X,1+Y,3/2-Z; [12]+X,1+Y,+Z; [13]+X,1-Y,1/2+Z; [14]1-X,-1+Y,3/2-Z; [15]+X,-1+Y,+Z; [16]+X,1-Y,-1/2+Z

Table S6. BVS results for the molybdenum atoms in **$Mo_{20}(ATMP)_4$** (left); **$Mo_{16}(EDTMP)_2$** (right).

Atom	BVS calc. for Mo	Atom	BVS calc. for Mo
Mo1	4.739	Mo1	4.828
Mo2	4.878	Mo2	5.036
Mo3	4.904	Mo3	4.925
Mo4	5.001	Mo4	4.888
Mo5	5.204	Mo5	5.117
		Mo6	4.866
		Mo7	4.877
		Mo8	5.220

Table S7 Proton conductivities of representative POM-based conducting crystalline materials.

Compounds	Proton conductivity (S/cm)	Temperature (°C)	RH (%)	Ref
$Mo_{20}(ATMP)_4$	**1.96×10^{-2}**	**85 °C**	**80%**	**This work**
$Mo_{16}(EDTMP)_2$	**4.17×10^{-3}**			
$NaH_{15}\{[P_2W_{15}Nb_3O_{62}]_2(4PBA)_2((4PBA)_2O)\}\cdot53H_2O$	1.59×10^{-1}	90 °C	98%	6
$[(AsW_9O_{33})_6\{W_2O_5(H_2O)(Ala)\}_2\{W_3O_6(H_2O)(Ala)\}_2\{W_2O_5(Ala)\}]$	2.83×10^{-4}	65 °C	75%	7
$[Ce_{11}Mo_{96}O_{286}(H_2O)_{101}(SO_4)_8]^{9-}$	9.01×10^{-2}	80 °C	98%	8
$H_{38}Na_{10}K_{14}(TMEDA)_8[Ln_{30}Ge_{12}W_{107}O_{420}(OH)_2(H_2O)_{14}]$	2.05×10^{-2}	85 °C	98%	9
$K_{11}Eu[P_5W_{30}O_{110}K]\cdot30H_2O$	1.0×10^{-2}	95 °C	90%	10
$H_2[Cu_2OL_3(H_2O)_2][Ce(L)(H_2O)_3(PW_{11}O_{39})]\cdot17H_2O$	3.175×10^{-4}	85 °C	98%	11
$H_4[CuL_3]_2[Ln(H_2O)_3(PW_{11}O_{39})]_2\cdot28H_2O$	1.750×10^{-4}			
$(n\text{-}Bu_4N)_6H_2[\{Mo_{24}O_{48}(OMe)_{32}\}\{Mo_{24}O_{52}(OMe)_{28}\}_2]\cdot25H_2O\cdot6CH_3CN$	6.73×10^{-6}	35 °C	98%	12
	1.79×10^{-3}	85 °C	98%	
$H\{Ln_4(L)_2(H_2O)_{21}[Zr_3(OH)_3(PW_9O_{34})_2]\}\cdot15H_2O$	7.53×10^{-3}	85 °C	98%	13
$[Cu(en)_2(H_2O)]_2[Cu(en)_2]_{10}H_{97}[Dy_{10}Nb_{190}]^{7-}$	1.19×10^{-4}	25 °C	98%	14
	3.75×10^{-3}	85 °C	98%	
$[NH_2(CH_3)_2]_{10}[Na_4(H_2O)_8]H_3[As_4W_{42}O_{142}(OH)_4(CH_3COO)_2Rh_3(H_2O)_4]\cdot13H_2O_4[NH(CH_3)_2]$	1.90×10^{-4}	25 °C	65%	15
$[K_4Na(H_2O)_6]KH_{10}[As_4W_{40}O_{140}Rh_4(H_2O)_4]\cdot34H_2O$	3.60×10^{-3}			

References

1. E. Cadot, B. Salignac, S. Halut and F. Sécheresse, *Angew. Chem. Int. Ed.*, 1998, **37**, 611-613.
2. A. O. Atsango, M. E. Tuckerman and T. E. Markland, *J Phys Chem Lett.*, 2021, **12**, 8749-8756.
3. O. V. Dolomanov, L. J. Bourhis, R. J. Gildea, J. A. K. Howard and H. Puschmann, *Journal of Applied*

Crystallography., 2009, **42**, 339-341.
4. H. Zang, H. N. Miras, J. Yan, D. L. Long and L. Cronin, *J Am Chem Soc*., 2012, **134**, 11376-9.
5. H. Chen, M. Zhang, Y. Li, P. Ma, J. Wang and J. Niu, Chem Commun., 2023, advance article, 10.1039/d3cc03645f.
6. S. Li, Y. Zhao, S. Knoll, R. Liu, G. Li, Q. Peng, P. Qiu, D. He, C. Streb and X. Chen, *Angew. Chem. Int. Ed*., 2021, **60**, 16953-16957.
7. K. Zheng, D. Yang, B. Niu, Y. Ye, P. Ma, J. Wang and J. Niu, *Inorg Chem*., 2022, **61**, 20222-20226.
8. X. X. Li, C. H. Li, M. J. Hou, B. Zhu, W. C. Chen, C. Y. Sun, Y. Yuan, W. Guan, C. Qin, K. Z. Shao, X. L. Wang and Z. M. Su, *Nat Commun*., 2023, **14**, 5025.
9. Z. Li, Z.-H. Lv, H. Yu, Y.-Q. Sun, X.-X. Li and S.-T. Zheng, *CCS Chemistry*., 2022, **4**, 2938-2945.
10. T. Iwano, K. Shitamatsu, N. Ogiwara, M. Okuno, Y. Kikukawa, S. Ikemoto, S. Shirai, S. Muratsugu, P. G. Waddell, R. J. Errington, M. Sadakane and S. Uchida, *ACS Appl Mater Interfaces*., 2021, **13**, 19138-19147.
11. R.-T. Zhang, H.-P. Xiao, Z. Li, M. Wang, Y.-F. Xie, Y.-D. Ye, X.-X. Li and S.-T. Zheng, *CrystEngComm*., 2021, **23**, 2973-2981.
12. Y. Wang, X. Ma, G. Li, H. Li, Q. Wang, W. Chen, P. Ma, S. Li, J. Niu and J. Wang, *Chemistry*., 2022, **28**, e202200637.
13. Y. H. Fan, M. Du, Y. X. Li, W. J. Zhu, J. Y. Pang, Y. Bai and D. B. Dang, *Inorg Chem*., 2022, **61**, 13829-13835.
14. R. D. Lai, J. Zhang, X. X. Li, S. T. Zheng and G. Y. Yang, *J Am Chem Soc*., 2022, **144**, 19603-19610.
15. Z. Liu, W. Wang, Y. Zhao, Z. Jing, R. Wan, H. Li, P. Ma, J. Niu and J. Wang, *Inorg Chem*., 2022, **61**, 15310-15314.